Biophysical Chemistry 170 (2012) 34–41

Contents lists available at SciVerse ScienceDirect

Biophysical Chemistry

journal homepage: http://www.elsevier.com/locate/biophyschem

Salt induced thermodynamic instability, concentration heterogeneity and phase transitions in lysozyme solutions

S.P. Rozhkov *, A.S. Goryunov

Institute of Biology, Karelian Research Center RAS, Pushkinskaya 11, 185910, Petrozavodsk, Russia

HIGHLIGHTS

- Dipole-dipole widening of ESR spectra of spin labeled lysozyme molecule is indicative of protein intermolecular interactions.
- Salt-induced concentration heterogeneity of lysozyme solution has been revealed.
- An analysis of the heterogeneity on the basis of lysozyme phase diagram has been provided.
- A theoretical substantiation of the salt-induced sol-gel transition in protein solution has been described.

GRAPHICAL ABSTRACT

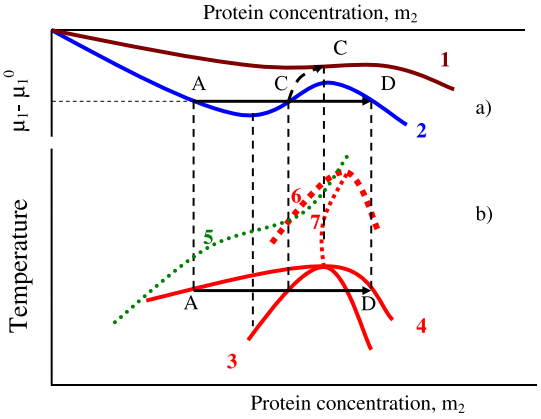

ARTICLE INFO

Article history:
Received 16 May 2012
Received in revised form 20 August 2012
Accepted 21 August 2012
Available online 28 August 2012

Keywords:
Dipole–dipole interaction of spin-labels
Protein clusters
Sol–gel transition
Phase diagram
Supercritical phase transition
Lysozyme

ABSTRACT

The ESR spin label method was used to estimate an average distance between spin-labeled protein molecules at a concentration of 35 mg/ml in solutions which contained 0 to 3 M NaCl. Three NaCl concentration ranges, in which the distance between protein molecules varied markedly, were revealed: the distance increased in the range 0 to 0.15 M NaCl, decreased in the range 0.3 M to 1.5 M NaCl and increased again in the range 1.5 M to 3 M NaCl. In lysozyme solutions, which contained 0.3 to 1.5 M NaCl, solution heterogeneity was observed to increase gradually during 4 days because of the emergence of supramolecular organization in the form of clusters and aggregates. Viscous gel was formed immediately under salting-out conditions at 3 M NaCl, and remained unchanged during 4 days. The results obtained are discussed on the basis of a theoretical and experimental phase diagram of lysozyme solution with an emphasis on analysis of continuous supercritical phase transitions which give rise to various types of dynamic and/or equilibrium protein clusters.

1. Introduction

The number of publications, in which the emergence of various concentration heterogeneities and phases in globular protein solutions are discussed, has been steadily growing in the past few years. Examples of heterogeneities are either permanent or dynamic clusters of protein macromolecules (oligomers) about 10 nm in size [1,2], mesoscopic clusters tens to hundreds of nanometers in size [3–5] and higher-order kinetic aggregates and associates [6]. Examples of phases are dense liquid microscopic drops emerging occasionally as a result of liquid–liquid (L–L) phase transition [7–9], crystalline nuclei and microcrystals and gel formed as a result of protein salting-out [10]. These phenomena

* Corresponding author.
E-mail address: rozhkov@krc.karelia.ru (S.P. Rozhkov).

0301-4622/$ – see front matter © 2012 Elsevier B.V. All rights reserved.
http://dx.doi.org/10.1016/j.bpc.2012.08.001

are directly related to important issues of biotechnology, biology and medicine, such as the contribution of concentration heterogeneities to crystal nuclei formation [11], the pathogenesis of diseases related to protein condensation [12], the aggregation stability of pharmaceutical preparations [13,14] and the osmotic homeostasis control mechanisms of visceral liquids [15,16].

Of special interest are heterogeneities that arise shortly after protein solution and fast with respect to protein crystallization process, so they can form and be present continuously in protein solution. Some of these heterogeneities are identified by static and dynamic light scattering methods [4,5]. They are interpreted as relatively long-lived (seconds) mesoscopic protein clusters (hundreds of nanometers) formed under conditions consistent with the solubility curve domain on a phase diagram of temperature versus protein concentration. This domain is located above the L–L phase separation curve and critical point temperature (in the supercritical domain). They are formed in a certain protein concentration range, where their size does not depend on protein concentration. Other heterogeneities are interpreted as clusters-oligomers which comprise up to 10 protein molecules. They are identified using the SAXS and SANS methods in approximately the same domain of the phase diagram but in slightly saline or salt-free solutions. Interaction between protein molecules in clusters-oligomers is controlled by short-range molecular attraction and electrostatic repulsion mechanisms [1]. Some authors [1,17] understand them as equilibrium clusters, while others [18,19] as dynamic. Thus, although some methodical problems in the approaches used have been resolved [20], additional experimental physical methods can be employed to study concentration heterogeneities in protein solutions and to further analyze available data on the state of solution with heterogeneities on the basis of phase diagrams.

Lysozyme solutions have been studied in detail by various methods, including theoretical models, to elucidate the role of cluster formation in crystal growth mechanisms [1,7,8,10,21,22] and the role of salts in aggregation [23,24]. For this purpose, phase diagrams of solubility, containing binodal and spinodal lines which separate the unstable domains of the diagram from stable and metastable, were constructed. Experimental and theoretical approaches were also developed to relate various types of concentration heterogeneities to the phase diagram domains where they arise. This has provided a much better understanding of the reasons for and mechanisms of L–L phase transition in the binodal domain and formation of permanent protein clusters up to 10 nm in size [1].

The electron spin resonance (ESR) spin-labeling method was used earlier to assess changes in the states of water–salt serum albumin solutions upon phase transitions [25]. In the present paper, the method was applied to lysozyme solutions to estimate relative changes in the average distance between macromolecules caused by variations in salt concentration. The additional widening of ESR spectrum lines, which is due to the dipole–dipole interaction of the spin labels which modifies a protein molecule, is often used to estimate the distance between paramagnetic centers [26–29]. Widening in the ESR spectra of vitrified protein matrices can be revealed, if the distance between the paramagnetic centers is not more than 6–8 nm [26]. As the average distance between protein molecules in a dense phase (or a cluster) is 0.6–1 nm [5], the formation of clusters is expected to result in the widened ESR spectra of spin labels, as was observed in spin-labeled protein solutions frozen at 77 K. The advantage of such an experimental approach is that it clearly shows whether the concentration heterogeneities observed are protein-rich or protein-lean microvolumes.

Another important task of the present study was to discuss the data obtained on the various types of concentration heterogeneities and new phases, formed in some domains of the phase diagram for protein solutions, on the basis of the thermodynamic understanding of the behavior of the water chemical potential, depending on protein and NaCl concentration.

2. Theory

The disturbance of protein solution stability relative to the salt-induced concentration heterogeneity of protein can be assessed by analyzing the behavior of the water chemical potential $(\mu_1-\mu_1^0)=\varphi(m_2,m_3)$, where m_2 and m_3 are protein and salt concentrations, because $(\mu_1-\mu_1^0)$ characterizes thermodynamic solution stability. A phase diagram of water–salt protein solution in coordinates (water chemical potential $\Delta\mu_1=\mu_1-\mu_1^0$, protein concentration m_2) at constant salt concentration proposed in ref. [30] was constructed on the basis of virial coefficients. In this diagram, the dependence of the chemical potential is shown with regard for two terms of the virial expansion of osmotic pressure, which leads mathematically to the parabolic shape of the relationship (curve 1 in Fig. 1a). The descending negative branch of the parabola is consistent with the stable state of protein solution in a good solvent. Although the growing negative segment of the parabola is also consistent with the stable state of the solution, it indicates the growth of free energy and a decline in thermodynamic affinity between solution components. As a result, protein interaction is invigorated, and concentration fluctuations rise. At the intersection of the abscissa by the parabola, $\mu_1-\mu_1^0=0$, that is the protein solution is in equilibrium with a solid phase. The protein concentration, at which the abscissa is intersected, is expected to be close to saturation protein concentration and to be consistent with

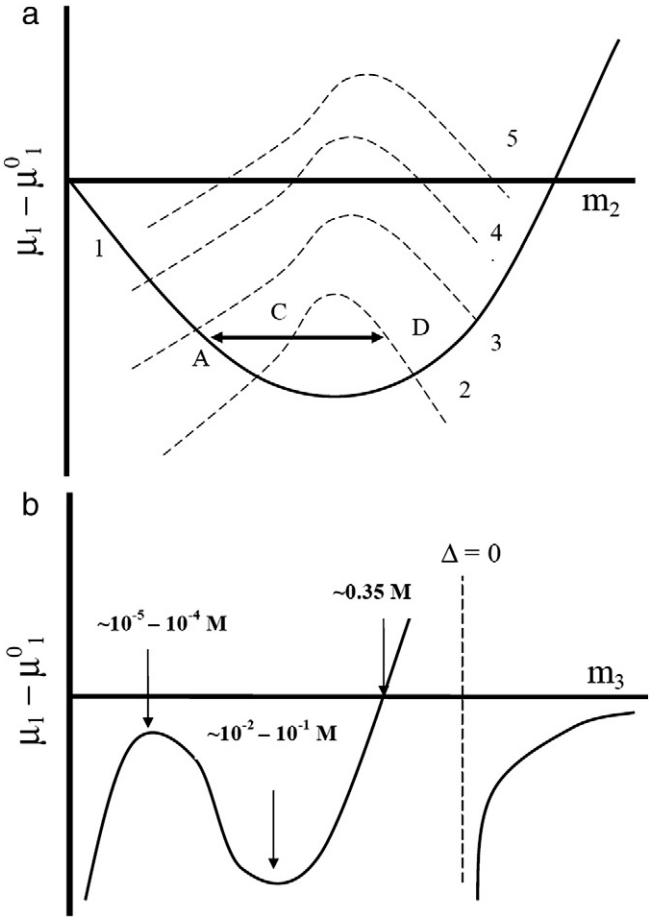

Fig. 1. a) Phase diagram of a system water–protein–salt in coordinates (chemical potential of water $\mu_1-\mu_1^0$, protein molar concentration m_2). Curve 1 (solid line) is an isotherm adapted from Arakawa and Timasheff [30]. Curves 2–5 (dashed line, Eq. (2)) characterize stability borders and correspond to different salt concentrations: from physiology important (2) to salting out (5). Below these curves the value of $\mu_1-\mu_1^0$ rises and a zone of instability exists (spinodal region). A→D characterizes metastable state of protein: dilute solution and dense liquid. b) Effect of salt concentration m_3 on water chemical potential $\mu_1-\mu_1^0$ estimated using Eq. (2) at constant protein concentration m_2. Arrows indicate approximate salt concentration range.

protein solubility. Position of curve 1 in Fig. 1a depends on temperature, salt concentration and salt type [30].

Protein solution typically loses its thermodynamic stability at high salt and protein concentrations, which corresponds to the domain where $\mu_1-\mu_1^0 \gg 0$. Transition from this state to a new, stable state with $(\mu_1-\mu_1^0)<0$ can lead to the formation of viscous gel, equilibrated presumably for a long time, or to the formation of crystalline phase.

Curve 1 in Fig. 1a (phase isotherm [30]) gives no opportunity to explain existence of experimentally observed L–L phase transition. We suggest that a "van der Waals loop" can occur on the isotherm $\mu_1-\mu_1^0=\varphi\ (m_2, m_3)$ as well as on isotherms for two-phase fluids in the phase transition zone. The isotherm follows the curve 1 in Fig. 1a until the intersection with the curve 2, follows the curve 2 until the next intersection with the curve 1 and then follows the curve 1 thus causing the formation of the loop for corresponding salt concentration. Stability boundaries for certain salt concentrations (dotted curves 2–5) were calculated analytically by integrating thermodynamic structural stability coefficient (Eq. (7) in ref. [31] or Eq. (3) in ref. [32]). Domain of the phase diagram below the "van der Waals loop" in Fig. 1a for each salt concentration is thermodynamically unstable relatively to protein concentration fluctuations (spinodal region). Arrow ACD indicates metastable equilibrium of dilute and dense protein phases (binodal).

Here we present an equation for "van der Waals loop" (stability boundary) as follows:

$$\mu_1-\mu_1^0 = -RT\frac{1+\Delta}{m_1\Delta z^2}\left\{\frac{2m_3}{\nu(2+\Delta)}\ln\left[4m_3^2(2+\Delta)-\Delta z^2 m_2^2\right] + \frac{4m_3^2}{\Delta z^2 a}\ln\frac{a+m_2}{a-m_2} - m_2\right\} \quad (1)$$

where $a^2=[4(2+\Delta)m_3^2/\Delta z^2]$.

In this equation, m_i is the molar concentration of water ($i=1$), protein ($i=2$) and salt ($i=3$); z is the protein charge; ν is the number of salt ions adsorbed on a protein molecule at specific sorption centers; $\Delta \approx -m_3\frac{\partial}{\partial m_3}\left(\frac{A\zeta^{1/2}}{1+r\kappa\zeta^{1/2}}-\Sigma\alpha_i\zeta^i\right)$ is the rate of variation in the activity coefficient of salt, where ζ is the ionic strength. Debye–Hückel expression for the activity coefficient of electrolyte, extended for higher salt concentrations by introducing empirical corrections α_i, is below the differentiation sign. As the activity coefficient for most salts decreases at first and then increases at higher concentration, the derivative of this function changes its sign. Therefore, Δ takes positive value at high salt concentrations and negative value at low salt concentrations.

For analytical clarity, the functions used in Eq. (1) can be conveniently presented as a power series expansion in terms of m_2 limited to third-power summand:

$$\mu_1-\mu_1^0 \approx RT\frac{1\pm\Delta}{m_1(2\pm\Delta)}\left\{\frac{m_2}{z^2}\mp\frac{2m_3}{\nu z^2\Delta}\ln 4m_3^2(2\pm\Delta)+m_2^2\frac{3m_3-m_2\nu}{6m_3^2\nu(2\pm\Delta)}\right\}+O(m^n) \quad (2)$$

where the upper sign in $(\pm,\mp)$ corresponds to $\Delta>0$ and the lower sign to $\Delta<0$. Although the parameter Δ is different for different salts and depends on their concentration, it is not more than one in value modulus. Therefore, only the sign before the second summand is essential:

$$\mp\frac{2m_3}{\nu\Delta z^2}\ln 4m_3^2(2\pm\Delta) \quad (3)$$

It follows from Eq. (2) that $\mu_1-\mu_1^0$ is uncertain at $m_3=0$ because we have m_3 in the numerator and logarithm of m_3 in the second summand. Analogously $\mu_1-\mu_1^0$ is uncertain at $z=0$.

At low salt concentration, the expression (3) which does not contain m_2, is preceded by the sign (+), and the value under the logarithm $4\ m_3^2(2\pm\Delta)$ is less than unity. Accordingly, $\mu_1-\mu_1^0<0$ that is consistent with stable states until $4\ m_3^2(2\pm\Delta)$ exceeds 1, i.e. until NaCl concentration exceeds 0.35 M. Increase in salt concentration at $4\ m_3^2(2\pm\Delta)>1$ will make the system increasingly unstable, because $\mu_1-\mu_1^0>0$. The concentration heterogeneity of the system will grow. As the parameter Δ approaches zero (~ at 1.6–2.0 M NaCl), $\mu_1-\mu_1^0\to+\infty$ and instability will increase until the sol–gel-type phase transition of the system takes place. As the parameter Δ passes through zero, jump-like gel formation will make the system more stable, because in this case $\mu_1-\mu_1^0\to-\infty$. However, the gel is unstable relative to the subsequent growth of salt concentration, because the modulus of the $\mu_1-\mu_1^0$ value decreases with the further growth of salt concentration because of the growth of Δ. Dependence of $\mu_1-\mu_1^0$ on concentration m_3 at a constant protein concentration m_2 is diagrammed in Fig. 1b in accordance with Eq. (2). It is interesting to note that in the range of physiological salt concentrations (~10^{-2} to

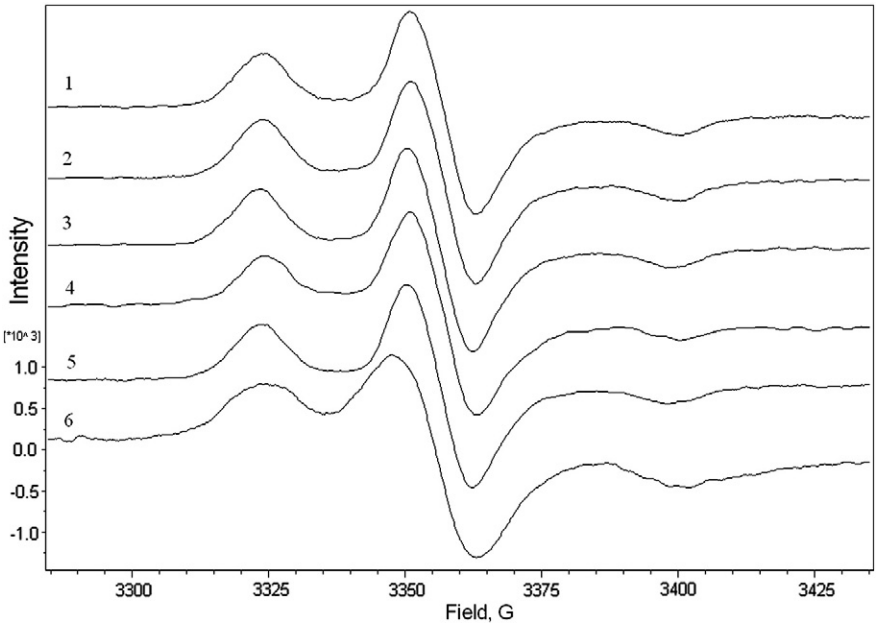

Fig. 2. ESR spectra of spin-labeled lysozyme at 77 K and SHF power 0.63 mW at different NaCl concentrations: 1–0 M; 2–0.03 M; 3–0.15 M; 4–0.75 M; 5–3.0 M. Bottom most spectrum (6) — 3.0 M NaCl and SHF power 12.6 mW.

10^{-1} M) this dependence has local minimum. Addition of salt in this range will lead to increase of $\mu_1 - \mu_1^0$ up to positive values at salting out concentrations. This is shown in Fig. 1a (curves 2–5 in order of increasing salt concentration).

3. Methods and materials

3.1. Spin-labelling

Lysozyme from hen egg white (Sigma) was modified by spin label 4-(2-iodoacetamido)-2,2,6,6-tetramethylpiperidine 1-oxyl (Takeda Chemical Industries), following the working procedure described in [33]. The spin label was incubated with lysozyme solution at pH 6.2 at 40 °C during 4 h. Histidine residue His-15 in lysozyme molecule was shown [33] to be selectively modified on protein under these conditions with the number of His-15 groups labeled about 0.8 mol/mol protein. The label which remained in the solution was removed by gel-filtration through a chromatographic column with sephadex G-25, using a 0.01 M phosphate buffer pH 6.4 as eluent. The protein solution was then concentrated, and various quantities of NaCl, dissolved in 0.01 M phosphate buffer, pH 6.4, were added. The final protein concentration in samples was 35 mg/ml.

ESR spectra were recorded using an ESR-spectrometer Bruker EMX at a modulation of 100 kHz and amplitude of 1 Gauss. A standard flat cuvette was used at room temperature and a cylindrical quartz cuvette at 77 K. Before taking spectra, the samples were kept for 6–8 h at 20 °C to induce the formation of the possible structural pattern of the solution, and changes in solution turbidity were then controlled visually during 4 days. The correlation times τ_c of spin-labeled protein were estimated at 20 °C at different salt concentrations, using formulas for fast radical rotation and the relation of the amplitudes of the low-field spectrum line to the central line and the central line width [26].

A temperature of 77 K in the sample was established by routinely flash-cooling of the cuvette with protein solution in liquid nitrogen. We suppose that the rearrangement of heterogeneous solution structure is prevented during the flash-freezing because the translational diffusion of molecules, coupled with overcoming of considerable potential barriers, is the limiting factor of the heterogeneities preservation [34].

4. Results

The amplitudes of the spectrum outer components d_1 and central component d and their ratio were estimated for samples, which differed in salt content, at 77 K (Fig. 2), depending on SHF-power. The parameter d_1/d, which is sensitive to the dipole–dipole interaction of nitroxyl radicals, can be used at a nitroxyl radical concentration in excess of 7×10^{-3} M to assess changes in the average distance between the spin labels [26] and, accordingly, between protein molecules spin-labeled at His-15 site. As the concentration of nitroxyl radicals decreases, the parameter d_1/d becomes less sensitive to the distance between them [27]. At a concentration of nitroxyl radical less than 7×10^{-3} M the shape of the SHF signal saturation curve can be used to assess their interaction [26]. The shape of the ESR spectrum in the absence of saturation and, hence, the d_1/d ratio depend primarily on the spin-spin relaxation time, T_2, and the course of the saturation curve depends equally on the value T_2 and on the spin–lattice relaxation time T_1. As T_1 is greater, it is more sensitive to paramagnetic interaction than T_2, and the use of saturation curves for assessing the long-distance interactions of spin labels can, therefore, make the method more sensitive.

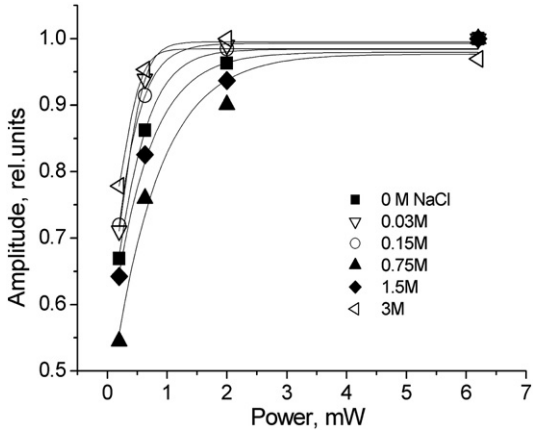

Fig. 3. Normalized amplitude values of the central component of the ESR spectrum of spin-labeled lysozyme, depending on saturating SHF power at various NaCl concentrations in protein solutions. Lines are guides for the eye.

Fig. 3 shows the amplitudes of the central line of the ESR spectrum of spin-labeled lysozyme obtained at 77 K at different NaCl concentrations, depending on SHF field intensity, in comparison with a control protein sample in 0.01 M phosphate buffer in the absence of NaCl (0 M NaCl). Based on a signal saturation pattern, the salt concentration range m_3 can be divided into three parts: (1) $0<m_3<0.15$ M; (2) 0.3 M$<m_3<$1.5 M; (3) $m_3>1.5$ M. At low salt concentrations (1) the saturation curve is less gently sloping than in the control sample, at medium concentrations (2) more gentle than in the control sample, and under salting-out conditions (3) less gentle again. More gently sloping saturation curves were shown [26] to be consistent with the more closely-spaced arrangement of spin labels. The shape of the saturation curve can thus be used to assess changes in the average distance between the labels $\boldsymbol{l}$. Consequently, in the first part of the salt concentration range the distance $\boldsymbol{l}$ between the spin labels is assumed to be greater than in the control sample, in the second part smaller and in the third part greater again.

Variations in the d_1/d ratio at varying SHF-power, at various salt concentrations and at 77 K are shown in Fig. 4. As SHF power increases, ESR signal parameters are observed to change (Fig. 2). The width and amplitude of the spectral components increase and the increment of the outer peak amplitude (d_1) is greater than that of the central peak amplitude (d). Differences between the d_1/d values of spin-labeled lysozyme solutions, containing different salt concentrations, can thus be revealed. In Fig. 5, these differences are shown for two SHF power values, 12.4 and 0.63 mW, obtained at different NaCl concentrations. In the absence of saturation (0.63 mW), d_1/d depends slightly on salt concentration, while at moderate saturation (12.4 mW) the dependence is more substantial. If the d_1/d ratio is used to estimate the average distance $\boldsymbol{l}$ between nitroxyl radicals $d_1/d \sim \boldsymbol{l}^{-1}$, then Figs. 3 and 5 show the following changes in the average distance $\boldsymbol{l}$ between protein-conjugated spin labels. As salt concentration rises to 0.15 M, the distance increases, then decreases and then increases again on achieving a NaCl concentration of 3 M (salting-out concentration). The formation of white viscous gel upon the salting-out of lysozyme is a well-known effect [7,10], which the authors observed before immersing the sample into liquid nitrogen.

These results, together with the fact that at a total spin label (and spin-labeled protein) concentration of 2.5×10^{-3} M the parameter d_1/d remains sensitive to varying conditions and SHF-power, show that concentration heterogeneities, in which local concentration is over 7×10^{-3} M, are formed in lysozyme solution.

A protein sample was immediately transformed to gel upon adding 3 M NaCl and remained as white gel during 4 days at 20 °C, while protein samples, which contained less than 0.3 M NaCl, remained transparent. Distinct opalescence, possibly associated with crystal formation, was not observed on the first day and was only visible after 4 days in the samples which contained 0.3 to 1.5 M NaCl and was not detected in the samples with smaller salt concentrations in 4 days. The higher the initial NaCl concentration, the more visible is the opalescence. A gradual decrease in the distance between protein

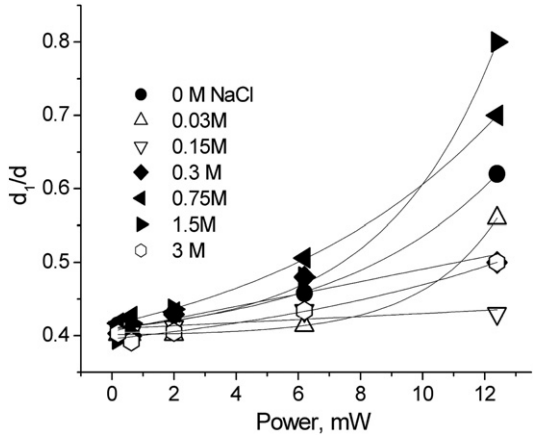

Fig. 4. ESR spectrum amplitude ratio values d_1/d, depending on SHF power at various NaCl concentrations. Lines are guides for the eye.

molecules over the range 0.3–1.5 M NaCl, revealed by analysis of the ESR spectra of spin-labeled lysozyme, is attributed to strong protein–protein interaction. This can give rise to various aggregates, dense-phase clusters and even crystalline-phase nuclei under these conditions [7,8,10]. However, as new-phase nuclei are commonly formed in several days, a decrease in distance in the range 0.3–0.8 M NaCl, inferred from ESR spectra after 6–8 h and not accompanied originally by visual opalescence, is assumed to be due to the formation of protein clusters and/or aggregates caused by the loss of the thermodynamic stability of the system.

In Fig. 6, the effective rotation correlation time of spin label against salt concentration at 20 °C is shown. Both the correlation time and the width of the central line of the spectrum increase monotonically over the entire salt range discussed. The correlation time (shown by a horizontal line 1 in Fig. 6) in salt-free solutions is greater than in low-salt solutions. ESR spectra give information first on the most fast type of label mobility, i.e. on own label mobility in water–protein matrix, rather than on the rotational dynamics of protein in general. So these variations in correlation time reflect changes in the microviscosity of a protein globule in the vicinity of spin label.

The first two points of both dependences shown in Fig. 6 are below the values corresponding to salt-free protein solution (solid horizontal lines 1 and 2). This indicates that at NaCl concentrations less than 0.15 M microviscosity declines slightly, which seems to be due to the loosening of protein globule structure in the vicinity of spin label under these conditions. However, both parameters increase subsequently at NaCl concentrations above 0.15 M, exceeding the salt-free solution level, which suggests the gradual salt-induced stabilization of protein structure in the vicinity of spin label. These changes are probably induced by some more vigorous interaction between protein molecules upon the formation of high-salt mesoscopic clusters and crystalline-phase nuclei.

A wide line appears in the ESR spectrum of spin-labeled lysozyme at the upper boundary of the range discussed at 3 M NaCl under salting-out conditions at 20°C, and correlation time increases substantially. A similar line is observed, for example, in 35% sucrose solution [35], suggesting a considerable increase in viscosity in the system. However, the average distance between spin labels on protein molecules does not diminish below the level observed at 0.3 M NaCl concentration (Fig. 5), as one could expect. This suggests that there is no crystalline phase in fresh gel and that gel is a cellular, fairly loose structure.

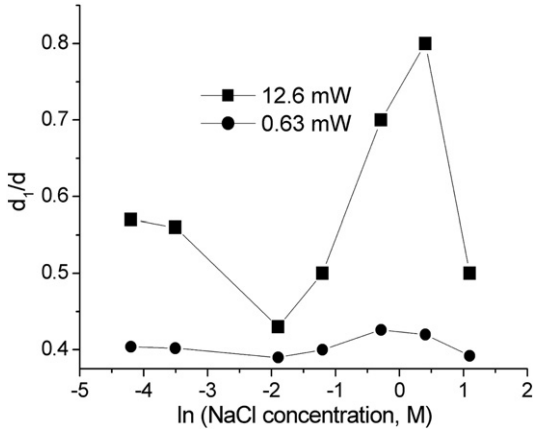

Fig. 5. Dependence of the parameter d_1/d on NaCl concentration (M) as ln(NaCl) at SHF power of 12.6 mW and 0.63 mW. The measurement error is smaller than symbol size.

5. Discussion

5.1. Effect of salt on solution destabilization

Shown in Fig. 7 is a semi-empirical phase diagram of lysozyme solution, which, together with the binodal lines (1–3) obtained earlier experimentally for fixed salt concentrations [7], contains an assumed binodal line for salt concentration 3M NaCl (curve 4). It has been shown in [7] that as salt concentration rises, the critical point of lysozyme solution is observed at increasingly elevating temperatures, so that the domain which was above binodal earlier is now at the binodal boundary. A phase transition of liquid–liquid type, connected with the formation of dense and dilute phases, is consistent with a binodal. Accordingly, in lysozyme solutions at low NaCl concentrations a binodal is expected to be in a low temperature range, and as salt concentration rises to 1.5 M at a protein content of 35 mg/ml, it is shifted to 20 °C and higher. As salt concentration continues to rise to 3M NaCl, viscous gel, rather than a concentrated but transparent phase (or dense-phase microdrops), is formed as a result of rapid kinetic spinodal decomposition [8,10]. The formation of white viscous gel is accompanied by an abrupt increase in correlation time (Fig. 6) indicating a decrease in the mobility of spin label. However, a relatively large distance between protein molecules, which remains unchanged with respect to that at 0.3 M NaCl (Figs. 3 and 5), suggests that the spatial net of gel is formed as a cellular fractal structure built of protein clusters due to intermolecular interactions of various origin [8].

No phase separation was observed in the physiological (0.15 M) salt concentration range during our experiments. Consequently, the experimental point, corresponding to 20 °C and 35 mg/ml of lysozyme, is above the binodal line (Fig. 7). However, dipole–dipole interaction of spin labels and the average distance between protein

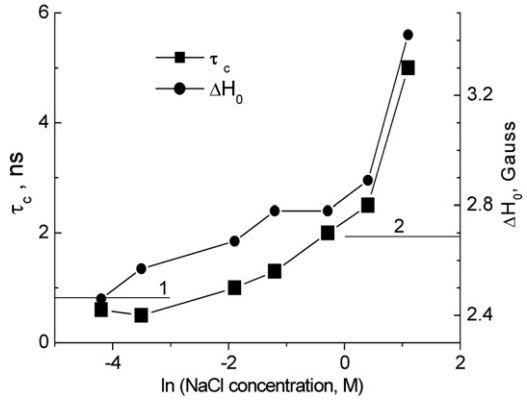

Fig. 6. Dependence of variation in the effective correlation time (τ_c) of the spin label, which modifies lysozyme molecules, and the width of the central component of the ESR spectrum (ΔH_0) on NaCl concentration (M) as ln(NaCl). τ_c and ΔH_0 values in salt-free protein solution are shown by horizontal line segments 1 and 2 accordingly. The measurement error is smaller than symbol size.

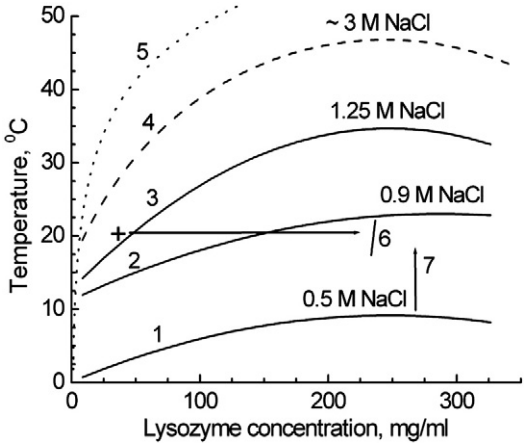

Fig. 7. Schematic phase diagram of lysozyme solution. 1–3-experimental binodals as phase equilibrium lines at corresponding NaCl concentrations according to ref. [7]. 4 — assumed binodal position at salt concentration 3 M NaCl. 5 — protein solubility line at 0.5 M NaCl according to [7]. 6 — assumed gel formation line at 3 M NaCl. Horizontal arrow indicates that experimental protein solution with lysozyme concentration 35 mg/ml (cross) and 3 M NaCl transforms into gel. Arrow 7 is an assumed quasi-spinodal for binodal 1. A mixture of protein clusters can be present in the supercritical phase transition domain between the solubility line (5) and binodals (1–3) because of the presence of quasi-spinodal 7. About 270 mg/ml protein correspond to the critical point. A small cross shows the temperature and protein concentration of the lysozyme solutions analyzed experimentally.

molecules are affected by salt both on lowering and rising salt concentration from 0.15 M NaCl. This is presumably due to concentration heterogeneities because protein (and label) concentration is 2.5×10^{-3} M. These heterogeneities are also identified using SANS and SAXS, in a phase diagram domain near the solubility line [1,5], and are interpreted as protein clusters. Theoretical estimation of $\mu_1-\mu_1^0=f(m_3)_{m2}$ (Fig. 1b) also predicts a decrease of solution stability at relatively low and high salt concentration that can result in clusters formation. Initial low-salt (10^{-5} to 10^{-4} M NaCl) decrease of stability may be caused by usual Debye–Hückel type electrostatic shielding and "salting out" effect of salt on apolar sites of protein surface which is known for lyophobic colloids. Another decrease of stability at high salt may be caused by the effect of preferential hydration [30]. Intermediate increase in thermodynamic stability in the range of physiological salt concentrations may be caused by adsorption of anions on protein surface leading to a decrease of specific surface energy (surface tension) and Gibbs free energy of mixing.

The authors assume that as NaCl is added, clusters of one type (type 1, up to 10 nm in size), which dominate in low NaCl solutions [1], are gradually replaced by other clusters (about 100 nm in size) formed upon addition of salts [5]. Fig. 6 shows that the correlation time of spin label rotation in the range of up to 0.1 M NaCl decreases relative to the low NaCl solution level, suggesting that such a transition from one type of clusters to another type is accompanied by the gradual transition of a protein globule to a looser, highly flexible structure. The probable reason for that is that as NaCl concentration rises, interaction between Cl^- ions and the sorption sites of a protein globule becomes more vigorous due to the increase of thermodynamic activity of salt ions with a rise in salt concentration. On the other hand, salt induced increase of surface tension is known to be an essential factor in protein structure stability owing to the mechanism of preferential hydration, but adsorption of ions gives generally an opposite result [36]. Chlorine anions are considered to be involved not only in the screening of positively charged groups but to be actively sorbed by the specific nonpolar zones of lysozyme and other protein molecules owing to the structure of their electronic shell and polarization capacity [37]. Up to ten such absorbed chlorine anions can exist [38].

However, at high salt concentrations, when adsorption sites are saturated, a rise in salt concentration results in the growth of specific surface energy, induced by preferential hydration effects [30], and in protein structure stabilization. This could also be due to a decline in thermodynamic solution stability relative to the emergence of concentration heterogeneity. Such a decline can be a result of more vigorous protein–protein interaction, indicated in the range 0.3–1.5 M NaCl by an increase in the correlation time of label rotation (Fig. 6), a decrease in the distance between protein molecules (Figs. 3 and 5) and a visual increase in solution turbidity observed after 4 days.

5.2. Effect of temperature on solution destabilization

Temperature is the most essential factor in the phase transition mechanism, and a critical point can be achieved by varying both composition and temperature. A possible relationship between the critical composition $X=(m_2/m_3)_{cr}$, consistent with the critical point and temperature can be obtained (see Fig. 2 in [32]).

The position of the characteristic points of the spinodal and binodal in the coordinates (chemical water potential, protein concentration) (Fig. 8a) and in the coordinates (temperature, protein concentration) (Fig. 8b) can be compared [39]. Curve 2 characterizes a family of isotherms for so low m_3 values that $\Delta<0$ (low salt limit). It has minimum and maximum points, which belong to the spinodal, and an inflection (maximum steepness) point which belongs to the quasi-spinodal [40]. Quasi-equilibrium A ↔ D of two phases with different protein concentration and the same chemical potential $\mu_1-\mu_1^0$ is presented by arrows in Fig. 8 a, b.

The important question regarding the dynamic nature of protein clusters revealed in the supercritical domain of the phase diagram for lysozyme solution is: are these clusters a thermodynamic or kinetic phenomenon? It is a problem which has not been completely resolved yet. The inflection points (C) on isotherm 2 (Fig. 8a) are indicative of a quasi-spinodal on the phase diagram. The theoretical prediction that quasi-spinodal temperature exceeds critical point temperature for the compositions $(m_2/m_3)>Q$ (low salt concentrations and/or high protein concentrations [32]) suggests that in this domain of the phase diagram corresponding phase transitions of supercritical type take place [40]. Phase transition of critical type, which takes place near the critical point of the phase diagram, can also be extended into a macroscopically homogeneous supercritical

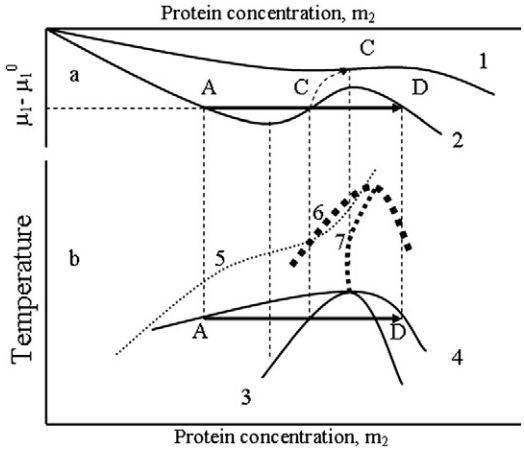

Fig. 8. Schematic representation of the phase diagram of a model water–protein–salt system showing water chemical potential isotherm ($\mu_1-\mu_1^0$) versus molar protein concentration m_2 (a) and temperature T versus protein concentration m_2 (b). Arrows indicate A–D phase quasi-equilibrium. Numbers indicate: 1 — supercritical isotherm for parameter $\Delta<0$; 2 — van-der-Waals type isotherm for parameter $\Delta<0$; 3 — spinodal; 4 — binodal; 5 — solubility curve; 6 — quasi-binodal and 7 — quasi-spinodal of supercritical fluid; C — maximum isotherm steepness point — point of quasi-spinodal. Critical point is the common point for spinodal, quasi-spinodal and binodal.

domain. Low stability is characteristic of the solution state in supercritical domain, and the lowest stability line is also a quasi-spinodal [40]. As there are only stable states in the quasi-spinodal domain, phases which have an interface do not co-exist there. In the quasi-spinodal domain concentration fluctuations are maximum, and the entire system is transformed into a mixture of fluctuation nuclei of both boundary phases (a mesophase state) without losing macroscopic heterogeneity [40].

Therefore, the existence of a theoretical quasi-spinodal provides an argument in favor of fluctuation phase transitions in the supercritical domain (in the solubility domain of the curve, above critical point temperature), which manifest themselves experimentally as dynamic protein clusters of nano- and mesoscopic sizes identified experimentally using high-precision physical methods [1,5]. Considering that the quasi-spinodal at $(m_2/m_3)_{cr} > Q$ lies between gel and solution [32], clusters formed as lysozyme oligomers, up to 10 nm in size, are assumed to be gel-like quasi-particles, and mesoscopic clusters to be fragments of the fractal aggregates of a gel phase formed of quasi-particles. As gel is formed immediately on adding excess salt, it would appear reasonable that there was a dynamic structure in the solution prior to gel formation and that this structure was related to mesoscopic cluster organization. In the quasi-spinodal domain, dynamic clusters can exist in a certain temperature range without being in equilibrium.

On one hand, if it is a quasi-spinodal, then there must be a quasi-binodal [40], i.e. conditions, under which metastable permanent protein clusters exist in apparently homogeneous solutions, are possible (Fig. 8b, curve 6). It is not surprising, therefore, that both static [1] and dynamic [18] protein clusters were discussed during the experiment in apparently the same domain of the phase diagram.

6. Conclusions

Salt-induced variations in the average distance between lysozyme molecules in the 0–3 M NaCl concentration range, accompanied by a probable increase in the flexibility of protein molecules at physiological salt concentrations and observed by the ESR spin labeling method, could be due to the passing of a water–protein–electrolyte system through the different domains of a phase diagram in supercritical and undercritical region. Being in thermodynamic unstable state with $\mu_1 - \mu_1^0 > 0$ at salt content above 0.3 M NaCl , the macroscopically homogeneous lysozyme solution represents a distinctive mesophase state understood as a system of the fluctuation fractal mesoscopic clusters of gel phase before crystalline-phase nuclei start to form. Most probably this domain of phase diagram may be presented as quasi-spinodal. However, at the assumed quasi-binodal boundary relatively stable permanent clusters — oligomers can exist at low salt concentrations and in salt less solutions. Salt induced sol–gel phase transition, which converts thermodynamically unstable system with $\mu_1 - \mu_1^0 \to +\infty$ into a gel state with $\mu_1 - \mu_1^0 \to -\infty$ takes place at the “salting-out” salt concentration above 1.6–2.0 M NaCl, where coefficient activity of salt has a minimal value. For future attempts we intend to carry out nanoparticle tracking analysis to investigate the size evolution of protein particles.

References

[1] A. Stradner, F. Cardinaux, P. Schurtenberger, A small-angle scattering study on equilibrium clusters in lysozyme solutions, The Journal of Physical Chemistry. B 110 (2006) 21222–21231.

[2] R. Piazza, Protein interacton and association: an open challenge for colloid science, Current Opinion in Colloid & Interface Science 8 (2004) 515–522.

[3] O. Glico, W. Pan, P. Katsonis, N. Neumaier, O. Galkin, S. Weinkauf, P.G. Vekilov, Metastable liquid clusters in super and undersaturated protein solutions, The Journal of Physical Chemistry. B 111 (2007) 3106–3114.

[4] P.G. Vekilov, Metastable mesoscopic phases in concentrated protein solutions, Annals of the New York Academy of Sciences 1161 (2009) 377–386.

[5] W. Pan, P.G. Vekilov, V. Lubchenko, Anomalous mesoscopic phases in protein solutions, The Journal of Physical Chemistry. B 114 (2010) 7620–7630.

[6] L.R. De Young, A.L. Fink, K.A. Dill, Aggregation of globular proteins, Accounts of Chemical Research 26 (1993) 614–620.

[7] M. Muschol, F. Rozenberger, Liquid–liquid phase separation in supersaturated lysozyme solutions and associated precipitate formation/crystallization, Journal of Chemical Physics 107 (6) (1997) 1953–1962.

[8] Y. Georgalis, P. Umbach, D.M. Soumpasis, W. Saenger, Dynamic and microstructure formation during nucleation of lysozyme solutions, Journal of the American Chemical Society 120 (1998) 5539–5548.

[9] N. Asherie, Protein crystallization and phase diagrams, Methods 34 (3) (2004) 266–272.

[10] A.C. Dumetz, A.M. Chockla, E.W. Kaler, A.M. Lenhoff, Protein phase behavior in aqueous solutions: crystallization, liquid–liquid phase separation, gels, and aggregates, Biophysical Journal 94 (2008) 570–583.

[11] C.N. Nanev, On slow protein crystal nucleation: cluster–cluster aggregation on diffusional encounters, Crystal Research and Technology 44 (2009) 7–12.

[12] S.E. Hill, J. Robinson, G. Matthews, M. Muschol, Amyloid protofibrils of lysozyme nucleate and grow via oligomer fusion, Biophysical Journal 96 (2009) 3781–3790.

[13] K. Ahrer, A. Buchacer, G. Iberer, A. Jungbauer, Thermodynamic stability and formation of aggregates of human immunoglobulin G characterized by differential scanning alorimetry and dynamic light scattering, Journal of Biochemical and Biophysical Methods 66 (2006) 73–86.

[14] H. Nishi, M. Miyajima, H. Nakagami, M. Noda, S. Uchiyama, K. Fukui, Phase separation of an IgG1 antibody solution under a low ionic strength condition, Pharmaceutical Research 27 (2010) 1348–1360.

[15] S.P. Rozhkov, Three-component system water–biopolymer–ions as a model of molecular mechanisms of osmotic homeostasis, Biophysics 46 (2001) 51–57.

[16] S.P. Rozhkov, Critical phenomena, phase equilibria, and structural temperature optimum of homeostasis in the water–biopolymer–electrolyte model system, Biophysics 50 (2005) 211–218.

[17] T. Fukasawa, T. Sato, Versatile application of indirect Fourier transformation to structure factor analysis: from X-ray diffraction of molecular liquids to small angle scattering of protein solutions, Physical Chemistry Chemical Physics 13 (2011) 3187–3196.

[18] A. Shukla, E. Mylonas, E. Di Cola, S. Finet, P. Timmins, T. Narayanan, D.I. Svergun, Absence of equilibrium cluster phase in concentrated lysozyme solutions, Proceedings of the National Academy of Sciences of the United States of America 105 (2008) 5075–5080.

[19] L. Porcar, P. Falus, W.-R. Chen, A. Faraone, E. Fratini, K. Hong, P. Baglioni, Y. Liu, Formation of the dynamic clusters in concentrated lysozyme protein solutions, Journal of Physical Chemistry Letters 1 (2010) 126–129.

[20] J. Trewhella, The different views from small angles, Proceedings of the National Academy of Sciences of the United States of America 105 (2008) 4967–4968.

[21] N. Niimura, Y. Minezaki, M. Ataka, T. Katsura, Aggregation in supersaturated lysozyme solution studied by time-resolved small angle neutron scattering, Journal of Crystal Growth 154 (1995) 136–144.

[22] K. Igarashi, M. Azuma, J. Kato, H. Ooshima, The initial stage of crystallization of lysozyme: a differential scanning calorimetric (DSC) study, Journal of Crystal Growth 204 (1999) 191–200.

[23] W. Liu, T. Cellmer, D. Keerl, J.M. Prausnitz, H.W. Blanch, Interactions of lysozyme in guanidinium chloride solutions from static and dynamic light-scattering measurements, Biotechnology and Bioengineering 90 (2005) 482–490.

[24] J. Rubin, A. San Miguel, A.S. Bommarius, S.H. Behrens, Correlation of aggregation kinetics and stationary diffusion in protein–sodium salt systems observed with dynamic light scattering, The Journal of Physical Chemistry. B 114 (2010) 4383–4387.

[25] S.P. Rozhkov, A.S. Goryunov, Effects of inorganic salts on the structural heterogeneity of serum albumin solutions, European Biophysics Journal 28 (2000) 639–647.

[26] G.I. Likhtenstein, Spin-labeling methods in molecular biology, Wiley, New York, 1976.

[27] A.M. Vasserman, A.L. Kovarski, Spin labels and probes in physical chemistry of polymers, Nauka, Moscow, 1986. [in Russian].

[28] P. Ionita, A. Caragheorgheopol, B.C. Gilbert, V. Chechik, Dipole–dipole interactions in spin-labeled Au nanoparticles as a measure of interspin distances, The Journal of Physical Chemistry. B 109 (2005) 3734–3742.

[29] K. Mevorat-Kaplan, L. Veiner, M. Sheves, Spin-labeling of *Natronomonas pharaonis* halorodopsin: probing the cysteine residues environment, The Journal of Physical Chemistry. B 110 (2006) 8825–8831.

[30] T. Arakawa, S.N. Timasheff, Mechanism of protein salting in and salting out by divalent salts: balance between hydration and salt binding, Biochemistry 23 (1984) 5912–5923.

[31] S.P. Rozhkov, Phase transitions and precrystallization processes in a water–protein–electrolyte system, J. Cryst. Growth 273 (2004) 266–279.

[32] S.P. Rozhkov, A.S. Goryunov, Thermodynamic study of protein phases formation and clustering in model water–protein–salt solutions, Biophysical Chemistry 151 (2010) 22–28.

[33] G.I. Likhtenstein, Yu.D. Ahmedov, L.V. Ivanov, L.A. Krinitskaja, Yu.V. Kohanov, Study of lysozyme molecule by spin label method, Molekularnaja Biologia 8 (1974) 48–54 (in Russian).

[34] S. Weber, T. Wolff, G. von Bunau, Molecular mobility in liquid and in frozen micellar solutions. EPR spectroscopy of nitroxide free radicals, Journal of Colloid and Interface Science 184 (1996) 163–169.

[35] A.I. Kaivarainen, S.P. Pozhkov, Determination of correlation times of lysozyme molecule and of the lysozyme–inhibitor complex at 5–30°C using spin label method, Biofizika 32 (1987) 22–25 (in Russian).

[36] K.D. Collins, Ion hydration: Implications for cellular function, polyelectrolytes, and protein crystallization, Biophysical Chemistry 119 (2006) 271–281.
[37] M. Bostrom, D.R.M. Williams, B.W. Ninham, Specific ion effects: why the properties of lysozyme in salt solutions follow a Hofmeister series, Biophysical Journal 85 (2003) 686–694.
[38] P. Retailleau, M. Ries-Kautt, A. Ducruix, No salting in of lysozyme chloride observed at low ionic strength over a large range of pH, Biophysical Journal 73 (1997) 2156–2163.
[39] A.A. Tager, Physical-chemistry of polymers, Nauchnyi Mir, Moscow, 2007. [in Russian].
[40] I.P. Bazarov, Thermodynamics, Vysshaja shkola, Moscow, 1983. [in Russian].